INTEGRAL TRANSFORM SOLUTION OF ABLATION PROBLEMS WITH PYROLYSIS

Daniel Fraga Sias, danielfs_7@hotmail.com
LTTC, PEM/COPPE/UFRJ – Mechanical Engineering Dept. – Universidade Federal do Rio de Janeiro, RJ, 21945-970

Nerbe J. Ruperti Jr., nruperti@cnen.gov.br
Comissão Nacional de Energia Nuclear – CNEN – Rua Gal. Severino, 90 CEP 22294-900 Rio de Janeiro, RJ

Renato Machado Cotta, cotta@mecanica.coppe.ufrj.br
LTTC, PEM/COPPE/UFRJ – Mechanical Engineering Dept. – Universidade Federal do Rio de Janeiro, RJ, 21945-970

Abstract. *This work is aimed at further advancing a computational procedure for the design of thermal protection systems of space vehicles during atmospheric reentry. The Generalized Integral Transform Technique is thus employed in obtaining a hybrid numerical-analytical solution for ablation problems with pyrolysis effects, assumed to occur at a specified temperature range. The Coupled Integral Equations Approach is employed in lumping the heat conduction problem within the region affected by pirolysis, and yielding a formulation of a single region transient heat conduction, for the virgin material, with both the pyrolysis and the ablative moving boundaries. The proposed approach is demonstrated for a previously studied benchmark case, numerically solved by the finite element method for the full local model, using typical thermophysical properties of composite thermal protection materials. Finally, the constructed code is verified against another model, also previously developed, for materials that do not undergo pyrolysis, by setting the pyrolysis heat equal to zero.*

Keywords*: Integral transforms, hybrid methods, ablation, pyrolysis, heat conduction, thermal protection*

Nomenclature

T_p^*	- Pyrolysis temperature
T_{ab}^*	- Ablation temperature
T	- Temperature
L	- Plate thickness
q	- Heat flux
k	- Thermal conductivity
cp	- Specific heat
ρ	- Density
$s(t)$	- Moving boundary position
H	- Latent heat
t	- Time
$\bar{T}pp_i(t)$	- Transformed potential in pré-pyrolysis period
$\bar{T}p_i(t)$	- Transformed potential in pyrolysis period
$\bar{T}a_i(t)$	- Transformed potential in ablation period

Greek letters

α	- Thermal diffusivity
βpp_i	- Eigenvalues in pré-pyrolysis period
$\beta p_i(t)$	- Eigenvalues in pyrolysis period
$\beta a_i(t)$	- Eigenvalues in ablation period
$\Psi pp_i(x)$	- Eigenfunctions in pré-pyrolysis period
$\tilde{\Psi} p_i(x,t)$	- Eigenfunctions in pyrolysis period
$\tilde{\Psi} a_i(x,t)$	- Eigenfunctions in ablation period

Subscripts

ab	- relates to ablation
av	- relates to average
p	- relates to pyrolysis
o	- relates to initial value
v	- relates to virgin material

1. INTRODUCTION

The design of recoverable orbital platforms requires the detailed analysis of the heat transfer process during the atmospheric reentry portion of the flight, involving the aerodynamic heating estimation and the determination of the heat absorbed by the vehicle surface and its interaction with the thermal protection system (TPS), either of the ablative or rejection type (Tauber, 1989, Bouilly et al., 1998, Amundsen et al., 2000). Such analysis is in general aimed at optimizing the TPS weight while the structure integrity is warranted, according to the thermal restrictions on the payload internal environment (Chen & Milos, 1999).

Besides the accurate characterization of the materials thermophysical properties, there is the need of constructing a robust, precise and computationally fast simulation tool, so as to reproduce the complex heat transfer process that occurs under such extreme conditions. Such a tool should be able to solve heat conduction problems with high heat flux levels, in order to allow for an optimized design of the thermal protection system. Not only the model should encompass the major physical phenomena, but the solution procedure itself should have a controllable accuracy, in light of the short steep transients and large thermal gradients that are typical of this class of problems.

Previous studies on ablative thermal protection systems have addressed the hybrid numerical-analytical solution via integral transforms of ablation controlled heat conduction (Ruperti & Cotta, 1991, Cotta, 1993, Cotta & Mikhailov, 1997, and Cotta, 1998, Gomes et al., 2006), aimed at producing accurate benchmark results for moving boundary problems typical of ablative TPS. More recently, improved lumped differential formulations have been proposed towards the simplification of the traditional local formulations of ablation problems, which were particularly useful in the development of design codes for the optimization of TPS thicknesses in typical reentry flights (Cotta et al., 1992, Ruperti Jr. & Cotta, 2000; Cotta et al., 2001, Cotta et al., 2004, Cotta et al., 2006).

While the approximate lumped formulations are indeed quite cost effective, it is also meritable to seek the computational enhancement in terms of processing time, for the more accurate approaches that address the solution of the original partial differential equations in this class of problems. Thus, Sias et al. (2005) employed a convergence acceleration approach to provide integral transform solutions of the ablation process within reasonable computational costs for TPS optimization purposes. Afterwards (Sias et al., 2007) this approach was applied to a more realistic ballistic reentry flight configuration, again employing the so-called integral balance technique to speed up the convergence of the proposed eigenfunction expansions.

Pyrolysis is the chemical decomposition of a condensed substance by heating. Extreme pyrolysis, which essentially leaves only carbon as the residue, is called carbonization and is also related to the chemical process of charring. Such phenomena may occur in a number of composite thermal protection materials, especially those composed of resins and high temperature fillers, and should be modeled for a representative simulation of thermal protections that employ such class of materials. Following the developments in (Sias et al., 2007) the present work implements the ablative TPS problem solution by including the pyrolysis effects, assumed to occur within a known temperature range. The proposed model derives its basis from that proposed by (Hogge & Gerrekens, 1982), which also assumes a temperature range for the pyrolysis effects, but neglects the mass flow rate effects due to the gases production within the medium.

Thus, the present work reports the attempt of implementing an accurate treatment of the ablation problem with pyrolysis by making use of the Generalized Integral Transform Technique, but still to within a reasonable low computational cost, aimed at its utilization in a TPS design code (Cotta et al. 2004). For this purpose, a convergence acceleration technique was employed, which essentially reduces the number of terms required in the eigenfunction expansions. The technique is called the integral balance approach, and has been employed in several previous developments in heat and mass transfer (Scofano Neto et al., 1990, Leiroz & Cotta, 1990, Cotta, 1993). In addition the problem formulation is simplified within the region that undergoes pyrolysis, by implementing an improved lumped differential reformulation via the so called Coupled Integral Equations Approach (CIEA), (Cotta & Mikhailov, 1997; Ruperti & Cotta, 2000), which basically lumps the region where the material changes properties with respect to the virgin material characteristics due to pyrolysis. Thus, this region is reformulated as a boundary condition for the local conduction problem in the virgin TPS, which recognizes the advancement of two different fronts, the pyrolysis and ablation fronts.

3. ANALYSIS

We consider one-dimensional transient heat conduction within a slab, representing a layer of thermal protection material applied over the nose surface of space vehicles that undergo atmospheric reentry aerodynamic heating. As the wall heat flux increases through the increasingly denser atmosphere, the wall temperature reaches a certain level when pyrolysis starts occurring, with the thermal, mechanical and chemical degradation of the virgin material, and this front progressively moves into the TPS layer thickness. As the heat load progresses, the material that already went through pyrolysis initiates the ablation process itself, again after a certain temperature level, characterized by an ablation temperature, while the ablative recession boundary is represented by the energy balance at this moving interface.

Thus, the problem is formulated for three different stages in the time variable, a pre-pyrolysis period, when the temperatures within the virgin material are below the pyrolysis value, a pyrolysis period when this phenomenon is started but ablation is not yet present, and finally the ablation period, when pyrolysis and ablation are simultaneously active over the TPS. The first period is essentially formulated as a linear heat conduction problem, for which an analytical solution is readily obtainable via the classical integral transform method. The other two periods involve, respectively, one or two moving boundaries, which are to be determined together with the temperature fields, which turns these formulation nonlinear in nature, due to the a priori unknown domain limits. For solving the heat transfer problem within these regions, we shall recall the Generalized Integral Transform Technique (GITT) (Cotta, 1993, Cotta & Mikhailov, 1997, Cotta, 1998); for handling the more involved heat conduction problems. Also, the present contribution takes advantage of an improved lumped-differential reformulation tool, the Coupled Integral Equations Approach (CIEA), (Cotta & Mikhailov, 1997; Ruperti & Cotta, 2000), to rewrite the pyrolysis region conduction problem as an energy balance for the virgin material boundary condition within the pyrolysis and ablation periods. In this sense, the problem formulation is significantly simplified, since a local solution is required only for the virgin material, where the temperature gradients are most significant and the lumping type approaches become less accurate. Therefore, the problem formulation for the three periods in time is written as:

Pre-pyrolysis period

$$\rho_{\mathrm{v}} cp_{\mathrm{v}} \frac{\partial T_{\mathrm{v}}(x,t)}{\partial t} = k_{\mathrm{v}} \frac{\partial^2 T_{\mathrm{v}}(x,t)}{\partial x^2}, \qquad 0 < x < L;\ 0 < t < t_{\mathrm{p}}$$
$$T_{\mathrm{v}}(x,t) = T_o \ , \quad t = 0;\ 0 \le x \le L$$
$$\frac{\partial T_{\mathrm{v}}(x,t)}{\partial x} = 0, \quad x = 0;\ 0 < t < t_{\mathrm{p}}; \quad k_{\mathrm{v}} \frac{\partial T_{\mathrm{v}}(x,t)}{\partial x} = q_w(\mathrm{t}), \quad x = L;\ 0 < t < t_{\mathrm{p}} \tag{1a-d}$$

Pyrolysis period

$$\rho_{\mathrm{v}} cp_{\mathrm{v}} \frac{\partial T_{\mathrm{v}}(x,t)}{\partial t} = k_{\mathrm{v}} \frac{\partial^2 T_{\mathrm{v}}(x,t)}{\partial x^2}, \qquad 0 < x < s_{\mathrm{p}}(t);\ t_{\mathrm{p}} < t < t_{\mathrm{ab}}$$
$$\rho_{\mathrm{p}} cp_{\mathrm{p}} \frac{\partial T_{\mathrm{p}}(x,t)}{\partial t} = k_{\mathrm{p}} \frac{\partial^2 T_{\mathrm{p}}(x,t)}{\partial x^2}, \qquad s_{\mathrm{p}}(t) < x < L;\ t_{\mathrm{p}} < t < t_{\mathrm{ab}}$$
$$T_{\mathrm{v}}(x,t) = \tilde{T}_{\mathrm{p}}(x), \quad t = t_{\mathrm{p}};\ 0 \le x \le s_{\mathrm{p}}(t_{\mathrm{p}});\ T_{\mathrm{p}}(x,t) = T_{\mathrm{p}}^*, \quad t = t_{\mathrm{p}};\ s_{\mathrm{p}}(t_{\mathrm{p}}) = L \tag{2a-g}$$
$$\frac{\partial T_{\mathrm{v}}(x,t)}{\partial x} = 0, \quad x = 0;\ t_{\mathrm{p}} < t < t_{\mathrm{ab}}; \quad k_{\mathrm{p}} \frac{\partial T_{\mathrm{p}}(x,t)}{\partial x} = q_w(t), \quad x = L;\ t_{\mathrm{p}} < t < t_{\mathrm{ab}}$$
$$T_{\mathrm{v}}(x,t) = T_{\mathrm{p}}(x,t) = T_{\mathrm{p}}^*, \quad x = s_{\mathrm{p}}(t);\ t_{\mathrm{p}} < t < t_{\mathrm{ab}}$$

Energy balance at pyrolysis interface

$$\rho_{\mathrm{v}} H_{\mathrm{p}} \frac{ds_{\mathrm{p}}(t)}{dt} = k_{\mathrm{v}} \frac{\partial T_{\mathrm{v}}(x,t)}{\partial x} - k_{\mathrm{p}} \frac{\partial T_{\mathrm{p}}(x,t)}{\partial x}, \qquad x = s_{\mathrm{p}}(t);\ t_{\mathrm{p}} < t < t_{\mathrm{ab}}$$
$$s_{\mathrm{p}}(t) = L, \quad t = t_{\mathrm{p}} \tag{3a,b}$$

Ablation period

$$\rho_{\mathrm{v}} cp_{\mathrm{v}} \frac{\partial T_{\mathrm{v}}(x,t)}{\partial t} = k_{\mathrm{v}} \frac{\partial^2 T_{\mathrm{v}}(x,t)}{\partial x^2}, \quad 0 < x < s_{\mathrm{p}}(t);\ t > t_{\mathrm{ab}}$$
$$\rho_{\mathrm{p}} cp_{\mathrm{p}} \frac{\partial T_{\mathrm{p}}(x,t)}{\partial t} = k_{\mathrm{p}} \frac{\partial^2 T_{\mathrm{p}}(x,t)}{\partial x^2}, \quad s_{\mathrm{p}}(t) < x < s_{\mathrm{ab}}(t);\ t > t_{\mathrm{ab}}$$
$$T_{\mathrm{v}}(x,t) = \tilde{\tilde{T}}_{\mathrm{p}}(x), \quad t = t_{\mathrm{ab}};\ 0 \le x \le s_{\mathrm{p}}(t_{\mathrm{ab}}) \tag{4a-g}$$
$$T_{\mathrm{p}}(x,t) = T_{\mathrm{ab}}(x), \quad t = t_{\mathrm{ab}};\ s_{\mathrm{p}}(t_{\mathrm{ab}}) \le x \le s_{\mathrm{ab}}(t_{\mathrm{ab}}) = L$$
$$\frac{\partial T_{\mathrm{v}}(x,t)}{\partial x} = 0, \quad x = 0;\ t > t_{\mathrm{ab}};\ T_{\mathrm{p}}(x,t) = T_{\mathrm{ab}}^*, \quad x = s_{\mathrm{ab}}(t);\ t > t_{\mathrm{ab}}$$
$$T_{\mathrm{v}}(x,t) = T_{\mathrm{p}}(x,t) = T_{\mathrm{p}}^*, \quad x = s_{\mathrm{p}}(t);\ t > t_{\mathrm{ab}}$$

Energy balance at ablation interface

$$\rho_{\mathrm{v}} H_{\mathrm{p}} \frac{ds_{\mathrm{p}}(t)}{dt} = k_{\mathrm{v}} \frac{\partial T_{\mathrm{v}}(x,t)}{\partial x} - k_{\mathrm{p}} \frac{\partial T_{\mathrm{p}}(x,t)}{\partial x}, \qquad x = s_{\mathrm{p}}(t);\ t > t_{\mathrm{ab}}$$
$$s_{\mathrm{p}}(t) = \overline{s}_{\mathrm{ab}}, \qquad t = t_{\mathrm{ab}}$$
$$\rho_{\mathrm{p}} H_{\mathrm{ab}} \frac{ds_{\mathrm{ab}}(t)}{dt} = -q_w(t) + k_{\mathrm{p}} \frac{\partial T_{\mathrm{p}}(x,t)}{\partial x}, \qquad x = s_{\mathrm{ab}}(t);\ t > t_{\mathrm{ab}} \tag{5a-d}$$
$$s_{\mathrm{ab}}(t) = L, \qquad t = t_{\mathrm{ab}}$$

where $q_{\mathrm{w}}(t)$ is the wall heat flux at the TPS external surface due to aerodynamic heating, $\tilde{T}_{\mathrm{p}}(x)$ is the initial temperature distribution in the virgin material for the pyrolysis period, $\tilde{\tilde{T}}_{\mathrm{p}}(x)$ $\tilde{T}_{\mathrm{p}}(x)$ is the initial temperature

distribution in the virgin material for the ablation period, $T_{ab}(x)$ $\tilde{T}_p(x)$ is the initial temperature distribution in the pyrolysis region for the ablation period, and $\bar{s}_{ab}$ is the position of the pyrolysis interface in the beginning of the ablation period, as obtained from the solution of the previous period.

The pre-pyrolysis period is readily solved through the classical integral transform method (Cotta, 1993), adopting the following integral transform pair:

$$\bar{T}pp_i(t) = \int_0^L \Psi pp_i(x) T_v(x,t) dx \qquad \textit{Transform}$$
$$T_v(x,t) = \sum_{i=0}^{\infty} \frac{\Psi pp_i(x)}{Npp_i} \bar{T}pp_i(t) \qquad \textit{Inverse} \tag{6a,b}$$

where $\Psi pp_i(x) = \cos(\beta_i x)$ are the eigenfunctions obtained through separation of variables applied on the homogeneous version of problem (1), Npp_i are the norms, $\bar{T}pp_i(t)$ are the transformed potentials, and the eigenvalues index *i* starts from zero due to the second type boundary conditions on both ends of the medium. The transformed potentials are readily obtained in explicit form and the temperature in the virgin material for the pre-pyrolysis period is given by:

$$T_v(x,t) = T_{av}(t) + \frac{2}{L}\sum_{i=1}^{\infty} \cos(\beta pp_i x) \frac{\alpha_v}{k_v} \int_0^t q_w(t') e^{-a_v \beta_i^2 (t-t')} dt' \tag{7}$$

where βpp_i are the eigenvalues, and the contribution of the first eigenvalue, $\beta pp_0 = 0$, is already split as the average temperature evolution, $T_{av}(t)$, given as:

$$T_{av}(t) = \frac{1}{L \rho_v cp_v} \int_0^t q_w(t') dt' \tag{8}$$

In order to determine the time required for the pyrolysis initiation, t_p, we let $x = L$ in eq.(7), for the surface temperature value equal to the pyrolysis temperature, T_p^*, which corresponds to $T_v(L, t_p) = T_p^*$, and then t_p is computed from the following transcendental equation:

$$T_p^* = T_{av}(t_p) + \frac{2}{L}\sum_{i=1}^{\infty} \cos(\beta pp_i L)^2 \frac{\alpha_v}{k_v} \int_0^{t_p} q_w(t') e^{-a_v \beta pp_i^2 (t_p - t')} dt' \tag{9}$$

Once the pyrolysis initiation temperature has been identified, we need now to handle the pyrolysis period governing equations, eqs.(2) and (3). Here, we have chosen to simplify the problem formulation in the pyrolysis region, by employing a $H_{1,1}/H_{0,0}$ improved lumped formulation as provided by the Coupled Integral Equations Approach, CIEA (Cotta & Mikhailov, 1997; Ruperti & Cotta, 2000), resulting in an ordinary differential equation for the average temperature evolution within the pyrolysis region, and a modified equation for the pyrolysis interface movement. Thus, after the simple filtering for homogenization purposes, shown below:

$$T^*(x,t) = T(x,t) - T_p^* \tag{10}$$

eqs.(2,3) for the virgin material, pyrolysis region and pyrolysis moving boundary are rewritten as:

$$\rho_v cp_v \frac{\partial T_v^*(x,t)}{\partial t} = k_v \frac{\partial^2 T_v^*(x,t)}{\partial x^2}, \quad 0 < x < s_p(t);\ t_p < t < t_{ab}$$
$$\rho_p cp_p \left(L - s_p(t)\right) \frac{dT_{avp}(t)}{dt} = \frac{3}{2} q_w(t) + \left(\rho_p cp_p \frac{ds_p(t)}{dt} - \frac{3k_p}{L - s_p(t)} \right) \left(T_{avp}(t) - T_p^* \right), \quad t_p < t < t_{ab}$$
$$T_v^*(x,t) = \tilde{T}_p(x) - T_p^*, \quad t = t_p;\ 0 \le x \le s_p(t) \tag{11a-f}$$
$$T_{avp}(t) = T_p^*, \quad t = t_p;\ \frac{\partial T_v^*(x,t)}{\partial x} = 0, \quad x = 0;\ t_p < t < t_{ab};\ T_v^*(x,t) = 0, \quad x = s_p(t);\ t_p < t < t_{ab}$$

$$\rho_{\mathrm{v}} H_{\mathrm{p}} \frac{ds_{\mathrm{p}}(t)}{dt} = \frac{q_{\mathrm{w}}(t)}{2} - \frac{3k_{\mathrm{p}}}{L - s_{\mathrm{p}}(t)}\left(T_{\mathrm{avp}}(t) - T_{\mathrm{p}}^{*}\right) + k_{\mathrm{v}} \frac{\partial T_{\mathrm{v}}^{*}(x,t)}{\partial x}, \qquad x = s_{\mathrm{p}}(t);\ \ t_{\mathrm{p}} < t < t_{\mathrm{ab}}$$
$$s_{\mathrm{p}}(t) = L, \quad t = t_{\mathrm{p}} \tag{12a,b}$$

In attempting to solve eq.(11a) for the virgin material through integral transforms, it becomes evident that the eigenvalue problem is now a time-dependent one, which does not permit the decoupling integral transformation of the transient term. Thus, the ideas in the Generalized Integral Transform Technique (GITT) are recalled, (Cotta, 1993, Cotta & Mikhailov, 1997, Cotta, 1998), as will be briefly illustrated in what follows. The integral transform pair becomes:

$$\overline{T}p_i(t) = \int_0^{s_{\mathrm{p}}(t)} \tilde{\Psi}p_i(x,t)\, T_{\mathrm{v}}^{*}(x,t)\, dx \qquad \textit{Transform}$$
$$T_{\mathrm{v}}^{*}(x,t) = \sum_{i=1}^{\infty} \tilde{\Psi}p_i(x,t)\, \overline{T}p_i(t) \qquad \textit{Inverse} \tag{13a,b}$$

where a symmetric kernel has been adopted, and the normalized eigenfunctions, $\tilde{\Psi}p_i(x,t)$, are written as:

$$\tilde{\Psi}p_i(x,t) = \frac{\Psi p_i(x,t)}{\sqrt{Np_i(t)}}, \quad \Psi p_i(x,t) = \cos\left(\beta p_i(t) x\right) \tag{14ª,b}$$

and $Np_i(t)$ is the normalization integral and $\overline{T}p_i(t)$ are the transformed potentials in pyrolysis period, to be determined. The time-dependent eigenvalues due to the moving boundary are explicitly obtained as:

$$\beta p_i(t) = \frac{(2i-1)\pi}{2 s_{\mathrm{p}}(t)} \tag{15}$$

The integral transformation process as applied to eqs.(11a,c,e,f) above, then results in a coupled system of ordinary differential equations for the transformed temperatures in the virgin material:

$$\frac{d\overline{T}p_i(t)}{dt} + \sum_{j=1}^{\infty} A_{ij}(t)\, \overline{T}p_j(t) = 0, \quad i = 1, 2, \ldots, \ \textit{and} \ \ t_{\mathrm{p}} < t < t_{\mathrm{ab}}$$
$$\overline{T}p_i(t_{\mathrm{p}}) = \overline{f}p_i(t_{\mathrm{p}}) \tag{16a,b}$$

which are to be simultaneously solved with the equation for the average temperature in the pyrolysis region, eqs.(11b,d), and the equation for the pyrolysis interface position, eq.(12). In order to avoid the direct substitution of the inverse formula, eq.(13b), in the temperature space derivative required in eq.(12a), the integral balance approach was employed (Cotta & Mikhailov, 1997; Sias et al., 2005 e 2007), so as to accelerate convergence of this eigenfunction expansions for the temperature derivatives, resulting in the following improved expression for the pyrolysis interface movement:

$$\rho_{\mathrm{v}} H_{\mathrm{p}} \frac{ds_{\mathrm{p}}(t)}{dt} = \frac{q_{\mathrm{w}}(t)}{2} - \frac{3k_{\mathrm{p}}}{L - s_{\mathrm{p}}(t)}\left(T_{\mathrm{avp}}(t) - T_{\mathrm{p}}^{*}\right) +$$
$$\rho_{\mathrm{v}} c p_{\mathrm{v}} \sum_{j=1}^{\infty}\left(\frac{dI\tilde{\Psi}p_j(t)}{dt}\overline{T}p_j(t) - I\tilde{\Psi}p_j(t)\sum_{k=1}^{\infty} A_{jk}(t)\overline{T}p_k(t)\right), \qquad t_{\mathrm{p}} < t < t_{\mathrm{ab}}$$
$$s_{\mathrm{p}}(t_{\mathrm{ab}}) = L \tag{17a,b}$$

The coefficients in the transformed system are readily obtained in analytical form from the integral relations below, employing symbolic computation:

$$A_{ij}(t) = \beta p_i^2 \delta_{ij} + \int_0^{s_{\mathrm{p}}(t)} \tilde{\Psi}p_i(x,t)\frac{\partial \tilde{\Psi}p_j(x,t)}{\partial t}\, dx,$$
$$\overline{f}p_i(t) = \int_0^{s_{\mathrm{p}}(t)} \tilde{\Psi}p_i(x,t)(\tilde{T}_{\mathrm{p}}(x) - T_{\mathrm{p}}^{*})dx, \qquad I\tilde{\Psi}p_j(t) = \int_0^{s_{\mathrm{p}}(t)} \tilde{\Psi}p_j(x,t)\, dx \tag{18a-c}$$

Once the pyrolysis period transformed system, eqs.(11b,d), (16a,b) e (17a,b), has been numerically solved under controlled accuracy by the NDSolve routine of the *Mathematica* system, (Wolfram, 2005), one readily reconstructs the virgin material temperature distribution from the inverse formula, eq.(13b). In order to compute the time required for the onset of ablation, t_{ab}, one takes the lumped relation that provides the average temperature at the pyrolysis region, $T_{avp}(t)$, given by the $H_{1,1}$ approximation as:

$$T_{avp}(t) = \frac{1}{2}\left(T_p^* + T_p(L,t)\right) + \frac{L - s_p(t)}{12}\left(\left.\frac{\partial T_p(x,t)}{\partial x}\right|_{x=s_p(t)} - \frac{q_w(t)}{k_p} \right) \tag{19}$$

Then we let $T_p(L,t) = T_{ab}^*$, and t_{ab} is then computed from the formed transcendental equation. Once the ablation initiation is identified, we need to proceed towards the solution of the ablation period formulation. Again, the same improved lumped-differential reformulation is applied to the pyrolysis region, which is now bounded by the two moving boundaries, the pyrolysis and ablation interfaces. The same filtering is adopted, eq.(10), and eqs.(4,5) are rewritten as:

$$\begin{aligned}
&\rho_v cp_v \frac{\partial T_v^*(x,t)}{\partial t} = k_v \frac{\partial^2 T_v^*(x,t)}{\partial x^2}, \qquad 0 < x < s_p(t);\ t > t_{ab} \\
&\rho_p cp_p \left(s_{ab}(t) - s_p(t)\right)\frac{dT_{avp}^*(t)}{dt} = \frac{3}{2}q_w(t) + \rho_p cp_p\left(\frac{ds_p(t)}{dt} - \frac{ds_{ab}(t)}{dt}\right)T_{avp}^*(t) + \frac{6k_p}{s_{ab}(t) - s_p(t)}\left(T_{ab}^* + T_p^* - 2T_{avp}^*(t)\right),\ t > t_{ab} \\
&T_v^*(x,t) = \tilde{\tilde{T}}_p(x) - T_p^*, \qquad t = t_{ab};\ 0 \le x \le s_p(t); \quad T_{avp}^*(t) = \frac{1}{s_{ab}(t) - s_p(t)}\int_{s_p(t)}^{s_{ab}(t)} T_{ab}(x)dx,\ t = t_{ab} \\
&\frac{\partial T_v^*(x,t)}{\partial x} = 0, \quad x = 0;\ t > t_{ab};\ T_v^*(x,t) = 0, \quad x = s_p(t);\ t > t_{ab}
\end{aligned} \tag{20a-f}$$

$$\begin{aligned}
&\rho_v H_p \frac{ds_p(t)}{dt} = k_v \frac{\partial T_v(x,t)}{\partial x} - \frac{2k_p}{s_{ab}(t) - s_p(t)}\left(3T_{avp}^*(t) - 2T_p^* - T_{ab}^*\right), \quad x = s_p(t);\ t > t_{ab} \\
&s_p(t) = \bar{s}_{ab}, \qquad t = t_{ab} \\
&\rho_p H_{ab}\frac{ds_{ab}(t)}{dt} = -q_w(t) + \frac{2k_p}{s_{ab}(t) - s_p(t)}\left(2T_{ab}^* + T_p^* - 3T_{avp}^*(t)\right), \quad x = s_{ab}(t);\ t > t_{ab} \\
&s_{ab}(t) = L, \qquad t = t_{ab}
\end{aligned} \tag{21a-d}$$

Similarly to the solution of the pyrolysis period, a time-dependent eigenvalue problem is chosen, due to the moving pyrolysis interface, $s_p(t)$, and the Generalized Integral Transform Technique, GITT, (Cotta, 1993, Cotta & Mikhailov, 1997, Cotta, 1998), is again employed. The integral transformation pair is proposed as:

$$\begin{aligned}
&\bar{T}a_i(t) = \int_0^{s_p(t)} \tilde{\Psi}a_i(x,t)T_v^*(x,t)dx \qquad \textit{Transform} \\
&T_v^*(x,t) = \sum_{i=1}^{\infty} \tilde{\Psi}a_i(x,t)\bar{T}a_i(t) \qquad \textit{Inverse}
\end{aligned} \tag{22a,b}$$

where again a symmetric kernel was prefered in terms of the normalized eigenfunctions, $\tilde{\Psi}a_i(x,t)$, also given as in eq.(14), $\Psi a_i(x,t) = \cos\left(\beta a_i(t)x\right)$, and $Na_i(t)$ is the nome and $\bar{T}a_i(t)$ the transformed potentials for the ablation period, to be determined. The eigenvalues $\beta a_i(t)$, are then given by eq.(15).

The integral transformation procedure is applied to eqs.(20a,c,e,f) above, providing the following system of coupled ordinary differential equations for the transformed temperatures in the virgin material:

$$\begin{aligned}
&\frac{d\bar{T}a_i(t)}{dt} + \sum_{j=1}^{\infty} B_{ij}(t)\bar{T}a_j(t) = 0, \qquad t > t_{ab} \\
&\bar{T}a_i(t_{ab}) = \bar{f}a_i(t_{ab})
\end{aligned} \tag{23a,b}$$

which needs to be solved simultaneously with the equation for the average temperatue in pyrolysis region, eqs.(20b,d), and the equations for the movement of the pyrolysis and ablation interfaces, eqs.(21). Again, to avoid the use of the inverse formula in the temperature derivative within eq.(21a), the integral balance approach is applied (Cotta e Mikhailov, 1997; Sias et al., 2005 e 2007) so as to accelerate the convergence of this particular eigenfunction expansion which is expected to be slower than the temperature expansion. Obtém-se, então, a equação otimizada para a fronteira de pirólise:

$$\rho_{\mathrm{v}} H_{\mathrm{p}} \frac{ds_{\mathrm{p}}(t)}{dt} = -\frac{2k_{\mathrm{p}}}{s_{\mathrm{ab}}(t)-s_{\mathrm{p}}(t)}\left(3T^{*}_{\mathrm{avp}}(t)-2T^{*}_{\mathrm{p}}-T^{*}_{\mathrm{ab}}\right)+$$

$$\rho_{\mathrm{v}} cp_{\mathrm{v}} \sum_{j=1}^{\infty}\left(\frac{dI\tilde{\Psi}a_j(t)}{dt}\bar{T}a_j(t)-I\tilde{\Psi}a_j(t)\sum_{k=1}^{\infty}B_{jk}(t)\bar{T}a_k(t)\right), \quad x=s_{\mathrm{p}}(t);\ \ t>t_{\mathrm{ab}} \tag{24a,b}$$

$$s_{\mathrm{p}}(t_{\mathrm{ab}})=\bar{s}_{\mathrm{ab}}$$

The transformed coefficients are symbolically obtained from the integral relations below:

$$B_{ij}(t)=\beta a_i^2\delta_{ij}+\int_0^{s_{\mathrm{p}}(t)}\tilde{\Psi}a_i(x,t)\frac{\partial\tilde{\Psi}a_j(x,t)}{\partial t}dx,$$

$$\bar{f}a_i(t)=\int_0^{s_{\mathrm{p}}(t)}\tilde{\Psi}a_i(x,t)(\tilde{\tilde{T}}_{\mathrm{p}}(x)-T^{*}_{\mathrm{p}})dx, \quad I\tilde{\Psi}a_j(t)=\int_0^{s_{\mathrm{p}}(t)}\tilde{\Psi}a_j(x,t)dx \tag{25a-c}$$

4. RESULTS AND DISCUSSION

Numerical results were obtained to illustrate the approach here proposed, following the test case for ablation with pyrolysis effects, as presented in (Hogge & Guerrekens, 1982). The numerical solution of the transformed ODE systems was achieved by making use of the NDSolve routine in platform *Mathematica v5.2*, (Wolfram, 2005). In solving ODE´s, the function NDSolve by default uses the algorithm LSODA (Hindmarsh, 1983), alternating between Adams method (predictor-corrector of orders 1 to 12) and the backward differentiation method of Gear (Wolfram, 2005). The function NDSolve also allows the direct specification of a method to be used, which is particularly useful in the solution of systems that are a priori known to be stiff. The option "BDF" forces the use of the backward differentiation algorithm, with orders from 1 to 5, which is well-known for its robustness in the solution of stiff systems. A previous analysis of the different possible schemes in the function NDSolve (Sias et al., 2005), led us to the use of the option "BDF" in light of the marked stiffness of the resulting transformed systems in this eigenfunction expansion approach.

In order to allow for direct comparison with the results in (Hogge & Guerrekens, 1982), the following dimensionless variables have been computed and reported:

$$\Theta(\eta,\tau)=\frac{T(x,t)-T_0}{T^{*}_{\mathrm{p}}-T_0};\quad \eta=1-\frac{x}{L};\quad \tau=\frac{\alpha t}{L^2};\quad Q_{\mathrm{v}}(\tau)=\frac{L\,q_{\mathrm{w}}(t)}{k_{\mathrm{v}}(T^{*}_{\mathrm{p}}-T_0)};\quad \eta_{\mathrm{p}}(\tau)=1-\frac{s_{\mathrm{p}}(t)}{L};\quad \eta_{\mathrm{ab}}(\tau)=1-\frac{s_{\mathrm{ab}}(t)}{L} \tag{26}$$

The physical data adopted in (Hogge & Guerrekens, 1982), although with some questionable numerical values, have been here employed for comparison purposes, as summarized below:

$L=0.4\,cm$; $\rho_{\mathrm{v}}=0.00165\,{kg}/{cm^3}$; $\rho_{\mathrm{p}}=0.00133\,{kg}/{cm^3}$ $\rho_{\mathrm{v}}c_{P\mathrm{v}}=0.64\,{J}/{cm^3K}$; $\rho_{\mathrm{p}}c_{P\mathrm{p}}=0.424\,{J}/{cm^3K}$

$k_{\mathrm{v}}=2.13x10^{-3}\,{W}/{cm\,K}$; $k_{\mathrm{p}}=3.20x10^{-3}\,{W}/{cm\,K}$; $\rho_{\mathrm{v}}H_{\mathrm{p}}=711\,{J}/{cm^3}$; $\rho_{\mathrm{p}}H_{\mathrm{ab}}=4090\,{J}/{cm^3}$;

$T_{\mathrm{p}}=2355\,K$; $T_{\mathrm{ab}}=8367\,K$; $q_{\mathrm{w}0}=500\,{kW}/{cm^2}$

Also, Figure 1 illlustrates the thermophysical properties variation in the transition between the virgin material and pyrolysis region, as from the data in (Hogge & Guerrekens, 1982).

Table 1 ilustrates the convergence behavior of the pyrolysis interface position along the pyrolysis period, prior to the onset of ablation, relative to the outer surface of the slab, $1-\eta_{\mathrm{p}}(\tau)$, where the dimensionless time for the pyrolysis initiation has been determined as $\tau_{\mathrm{p}}=0.00026219$. This parameter was chosen to illustrate convergence in this period, in light of its importance in the design of thermal protection systems. One immediately concludes that the results for the dimensionless position of the pyrolysis front is converged to ±1 on the fifth significant digit up to *N=60*, and to much lower truncation orders, *N=20*, if three significant digits are considered sufficient for the prediction of this quantity, which might suffice for most design computational tools. Table 2 provides a direct comparison of these converged

results for the dimensionless interface position and its velocity, $\eta_p(\tau)$ and $\dot{\eta}_p(\tau)$, of the present GITT results and the numerical results of Hogge & Guerrekens(1982). From the columns that stand for the relative deviation between these two sets of results, we may observe the decreasing deviation between the two approaches as the pyrolysis front advances, for both the dimensionless position and velocity.

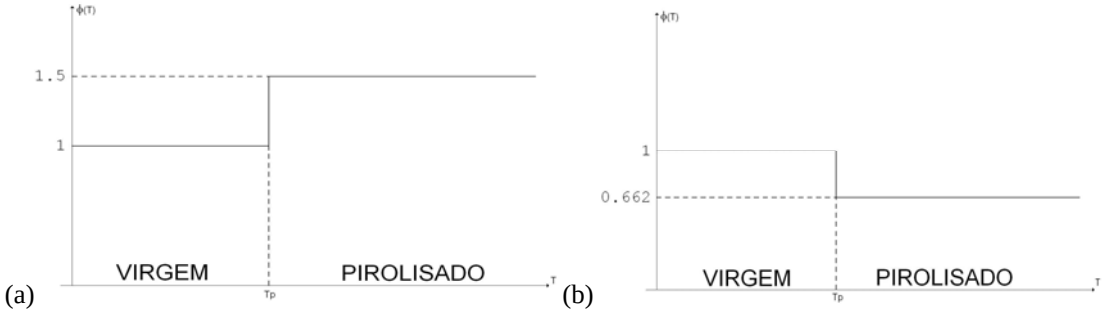

$k(T) = k_o \phi(T)$ $\qquad$ $\rho cp(T) = (\rho cp)_o \, \phi(T)$

Figure 1. (a) Thermal conductivity variation and (b) thermal capacity variation between virgin material and pyrolysis region (Hogge & Guerrekens, 1982).

Table 1 – Convergence of the solution for the pyrolysis interface position with respect to the outer surface, $1-\eta_p(\tau)$, along the pyrolysis period, for increasing truncation orders in the eigenfunction expansions.

Time	**Truncation order** N									
τ	**10**	**20**	**30**	**40**	**50**	**60**	**70**	**80**	**90**	**100**
.000959	.980870	.983950	.984658	.984828	.984883	.984905	.984915	.984920	.984925	.984925
.001655	.965027	.968332	.968945	.969095	.969142	.969165	.969173	.969178	.969180	.969183
.002352	.950683	.953785	.954335	.954475	.954518	.954538	.954545	.954550	.954553	.954555
.003048	.937295	.940153	.940663	.940793	.940833	.940850	.940857	.940862	.940865	.940868
.003745	.924622	.927275	.927753	.927873	.927913	.927927	.927935	.927940	.927945	.927942
.004441	.912533	.915023	.915475	.915588	.915625	.915640	.915648	.915653	.915655	.915655
.005138	.900940	.903298	.903730	.903838	.903873	.903888	.903895	.903898	.903900	.903903
.005834	.889780	.892030	.892443	.892547	.892583	.892595	.892603	.892605	.892608	.892610
.006531	.879005	.881163	.881560	.881660	.881693	.881708	.881713	.881717	.881717	.881720
.007227	.868567	.870648	.871032	.871130	.871160	.871172	.871180	.871183	.871185	.871188

Table 2 – Relative deviation between GITT solution with finite elements results (Hogge & Guerrekens, 1982) for the pyrolysis interface position and its velocity, $\eta_p(\tau)$ e $\dot{\eta}_p(\tau)$

Time	$\eta_p(\tau)$			$\dot{\eta}_p(\tau)$		
τ	*GITT - pyrolysis period*	*Hogge & Guerrekens(1982)*	*Relative deviation%*	*GITT - pyrolysis period*	*Hogge & Guerrekens(1982)*	*Relative deviation%*
0.001	0.01599	0.01376	16.21	0.57313	0.48986	17.00
0.002	0.03819	0.03193	19.61	0.43824	0.41742	4.99
0.003	0.05821	0.04888	19.09	0.39952	0.38484	3.81
0.004	0.07663	0.06702	14.34	0.37045	0.36013	2.87
0.005	0.09381	0.08462	10.86	0.34772	0.34344	1.25
0.006	0.11002	0.10095	8.98	0.32926	0.32869	0.17
0.007	0.12542	0.11600	8.12	0.31385	0.31153	0.74
0.008	0.14013	0.13099	6.98	0.30071	0.29940	0.44

Figure 2 graphically shows the behavior of the interface position and its velocity, $\eta_p(\tau)$ and $\dot{\eta}_p(\tau)$, as compared to the numerical solution of (Hogge & Guerrekens, 1982), computed for the full differential formulation of the problem, from the data in Table 2 above, where again we may notice the better agreement for the larger values of dimensionless time. Figure 3 shows the dimensionless average temperature distribution in the pyrolysis region, $\Theta_{avp}(\tau)$, again compared against the finite element results of (Hogge & Guerrekens, 1982) in dimensionless form. A truncation order of N=100 terms was employed in such simulations, though the results are converged to the graph scale at much lower

systems sizes. The agreement between the two independent solutions for the average pyrolysis region temperature is excellent, and provides the necessary confidence for the extension of the analysis towards the ablative period. Table 3 shows the numerical values for this comparison of the average pyrolysis region temperature, $\Theta_{avp}(\tau)$, and provides the estimates of the relative deviations between the two sets of results. One again observes a decreasing relative deviation as the pyrolysis interface progresses, and a maximum deviation of around 2% in this range of dimensionless time.

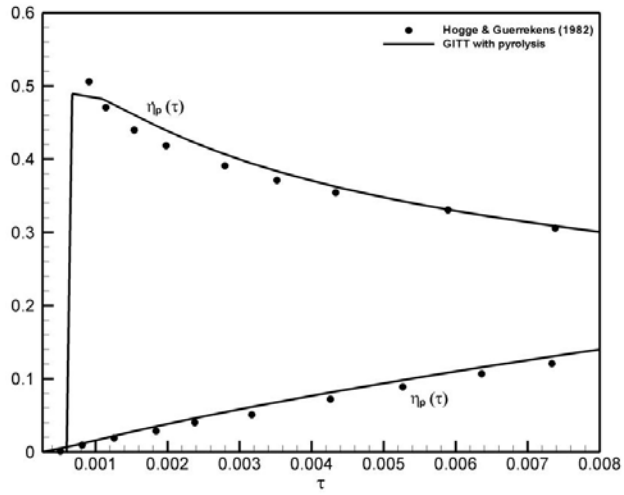

Figure 2. Comparison of GITT and finite element results for the pyrolysis interface position and its velocity, $\eta_p(\tau)$ and $\dot{\eta}_p(\tau)$, along the pyrolysis period.

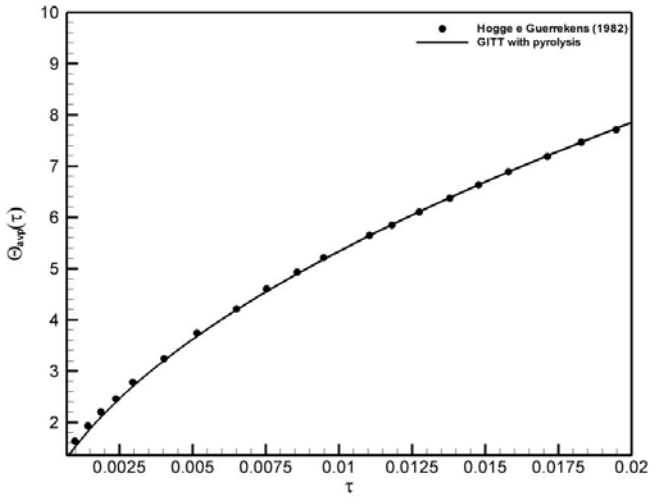

Figure 3. Comparison of GITT and finite element results for the dimensionless average pyrolysis region temperature, $\Theta_{avp}(\tau)$, along the pyrolysis period.

Table 3 – Relative deviation between GITT and finite element results for the dimensionless average pyrolysis region temperature, $\Theta_{avp}(\tau)$, along the pyrolysis period.

Tempo	$\Theta_{avp}(\tau)$		
τ	*GITT - pyrolysis period*	*Hogge & Guerrekens(1982)*	*Relative deviation%*
0.0025	2.46387	2.52036	-2.24
0.0050	3.61949	3.67786	-1.59
0.0075	4.54265	4.59697	-1.18
0.0100	5.33637	5.36292	-0.50
0.0125	6.04443	6.03849	0.10
0.0150	6.69032	6.69103	-0.01
0.0175	7.28837	7.27865	0.13
0.0200	7.84810	7.82049	0.35

Tables 4 and 5 illustrate the convergence behavior of the pyrolysis and the ablation interfaces positions along the ablation period, relative to the outer surface of the slab, $1-\eta_p(\tau)$ and $1-\eta_{ab}(\tau)$, where the dimensionless time for the ablation initiation has been determined as $\tau_{ab} = 0.007227$. Clearly, both interfaces positions are fully converged to six significant digits for truncation orders of N=45, and the lower truncation orders, N=12, already provide at least three fully converged significant digits, throughout the ablative period. Thus, it can be anticipated that fairly low truncation orders, and therefore low computational costs, can be achieved in the realm of application to an actual TPS optimization computational task.

Figure 4 illustrates the movement of the pyrolysis and ablation interfaces, since the beginning of the pyrolysis period, and compares the results obtained with GITT against those provided by (Hogge & Guerrekens, 1982). Both curves for $\eta_p(\tau)$ e $\eta_{ab}(\tau)$, show an overall good adherence with (Hogge & Guerrekens, 1982), but with a noticeable increasing deviation of the pyrolysis interface position for the larger times within the ablation period. Here, with the advancement of the ablation front, the temperature gradients within the pyrolysis region can be increasing significantly with the narrowing of the pyrolysis region, which makes the lumped formulation less accurate in this phase of the heat transfer process. Figure 5, which corresponds to the dimensionless interfaces velocities throughout the process, indicates that the velocity of the ablation front is also affected by the narrowing of the pyrolysis region at the later stages of the ablative period, with a more noticeable deviation between the two sets of results.

Table 4 - Convergence of the solution for the pyrolysis interface position with respect to the outer surface, $1-\eta_p(\tau)$, along the ablation period, for increasing truncation orders in the eigenfunction expansions.

Time	Truncation order N								
t	**12**	**23**	**34**	**45**	**56**	**67**	**78**	**89**	**100**
.007227	.871188	.871188	.871188	.871188	.871188	.871188	.871188	.871188	.871188
.007909	.861070	.861203	.861220	.861223	.861225	.861225	.861225	.861225	.861228
.008591	.851463	.851617	.851628	.851640	.851640	.851643	.851643	.851643	.851643
.009273	.842177	.842335	.842345	.842358	.842358	.842360	.842360	.842360	.842360
.009956	.833133	.833290	.833300	.833312	.833315	.833315	.833315	.833315	.833315
.010638	.824282	.824440	.824450	.824463	.824465	.824465	.824465	.824465	.824465
.011320	.815595	.815750	.815760	.815773	.815775	.815775	.815775	.815775	.815775
.012002	.807043	.807198	.807208	.807220	.807220	.807223	.807223	.807223	.807223
.012684	.798607	.798760	.798773	.798783	.798785	.798785	.798785	.798785	.798788
.013366	.790275	.790428	.790437	.790450	.790450	.790450	.790453	.790453	.790453
.014049	.782033	.782183	.782193	.782205	.782205	.782208	.782208	.782208	.782208

Table 5 - Convergence of the solution for the ablation interface position with respect to the outer surface, $1-\eta_{ab}(\tau)$, along the ablation period, for increasing truncation orders in the eigenfunction expansions.

Time	Truncation order N								
t	**12**	**23**	**34**	**45**	**56**	**67**	**78**	**89**	**100**
.007227	1.00000	1.00000	1.00000	1.00000	1.00000	1.00000	1.00000	1.00000	1.00000
.007909	.999560	.999553	.999550	.999550	.999550	.999550	.999550	.999550	.999550
.008591	.998383	.998368	.998365	.998365	.998365	.998365	.998365	.998365	.998365
.009273	.996630	.996617	.996615	.996615	.996615	.996615	.996615	.996615	.996615
.009956	.994415	.994407	.994405	.994407	.994407	.994407	.994407	.994407	.994407
.010638	.991823	.991818	.991815	.991818	.991818	.991818	.991818	.991818	.991818
.011320	.988905	.988908	.988905	.988908	.988908	.988908	.988908	.988908	.988908
.012002	.985710	.985718	.985718	.985720	.985720	.985720	.985720	.985720	.985720
.012684	.982275	.982288	.982285	.982290	.982290	.982290	.982290	.982290	.982290
.013366	.978623	.978640	.978640	.978645	.978645	.978645	.978645	.978645	.978645
.014049	.974783	.974805	.974803	.974808	.974808	.974808	.974808	.974808	.974808

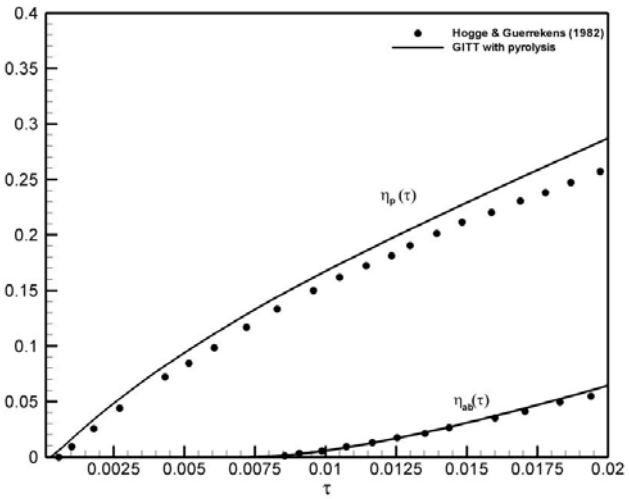

Figure 4. Comparison of GITT and finite element results for the pyrolysis and ablation interfaces positions, $\eta_p(\tau)$ and $\eta_{ab}(\tau)$, along the ablation period.

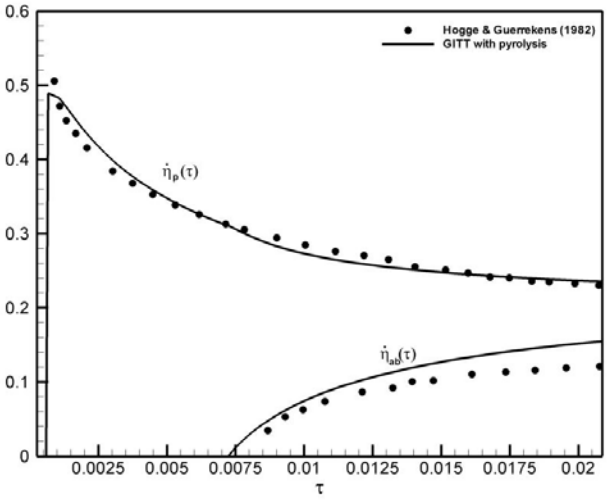

Figure 5. Comparison of GITT and finite element results for the pyrolysis and ablation interfaces velocities, $\dot{\eta}_p(\tau)$ and $\dot{\eta}_p(\tau)$, along the ablation period.

Tables 6 and 7 below quantify these deviations between the present GITT/CIEA solution against the numerical solution of the local model in Hogge & Guerrekens(1982), respectively, for the interfaces positions and velocities. It then becomes more evident the progressive increase in the deviations for both the interface positions and their velocities, as the ablation front moves inward, narrowing the pyrolysis region and promoting very large temperature gradients in this region.

Table 6 – Relative deviations between GITT solution and finite elements results (Hogge & Guerrekens, 1982) for pyrolysis and ablation interfaces positions, $\eta_p(\tau)$ and $\eta_{ab}(\tau)$, along the pyrolysis and ablation periods.

Time	$\eta_p(\tau)$			$\eta_{ab}(\tau)$		
τ	*GITT - pyrolysis and ablation periods*	*Hogge & Guerrekens(1982)*	*Relative deviation%*	*GITT - pyrolysis and ablation periods*	*Hogge & Guerrekens(1982)*	*Relative deviation%*
0.0025	0.04843	0.03976	21.81	-	-	-
0.0050	0.09382	0.08202	14.39	-	-	-
0.0075	0.13285	0.12152	9.32	-	-	-
0.0100	0.16727	0.15552	7.56	0.00575	0.00595	-3.36
0.0125	0.19895	0.18350	8.42	0.01676	0.01720	-2.56
0.0150	0.22916	0.21306	7.56	0.03082	0.03005	2.56
0.0175	0.25844	0.23559	9.70	0.04692	0.04410	6.39
0.0200	0.28706	0.25961	10.57	0.06450	0.05810	11.02

Table 7 – Relative deviations between GITT solution and finite elements results (Hogge & Guerrekens, 1982) for pyrolysis and ablation interfaces velocities, $\dot{\eta}_p(\tau)$ and $\dot{\eta}_{ab}(\tau)$, along the pyrolysis and ablation periods.

Tempo	$\dot{\eta}_p(\tau)$			$\dot{\eta}_{ab}(\tau)$		
τ	*GITT - pyrolysis and ablation periods*	*Hogge & Guerrekens(1982)*	*Relative deviation%*	*GITT - pyrolysis and ablation periods*	*Hogge & Guerrekens(1982)*	*Relative deviation%*
0,0025	0.41741	0.39975	4.42	-	-	
0,0050	0.34771	0.34362	1.19	-	-	
0,0075	0.30597	0.30863	-0.86	-	-	
0,0100	0.27316	0.28506	-4.17	0.07446	0.06321	17.80
0,0125	0.25733	0.26885	-4.28	0.10657	0.08804	21.05
0,0150	0.24783	0.25161	-1.50	0.12690	0.10315	23.02
0,0175	0.24139	0.24017	4.42	0.14116	0.11393	23.90
0,0200	0.23670	0.23238	1.19	0.15183	0.12011	26.41

A final verification of the implemented approach is provided by comparing the present results with the simulation of (Sias et al., 2007), also undertaken under a GITT/CIEA modeling, for materials that do not undergo pyrolysis, and ablation is the only recession front to be considered. In order to reproduce the results in (Sias et al., 2007), we let the pyrolysis heat to be null ($H_p = 0$) in the present code, and Figure 6 illustrates the perfect matching of the ablation interface position and velocity as computed through the two models, along the whole ablation period.

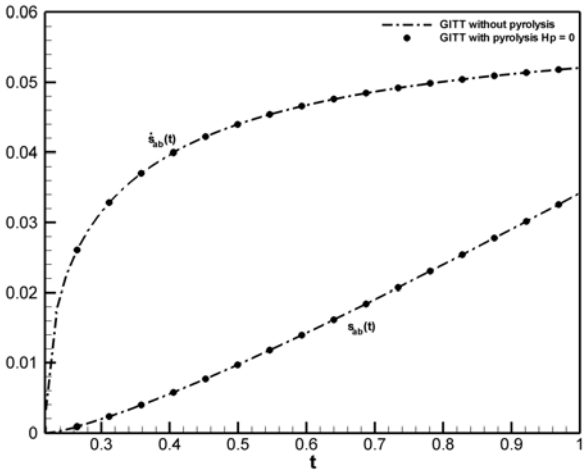

Figure 6. Comparison of model for materials without pyrolysis and present implementation with $H_p = 0$

5. ACKNOWLEDGEMENTS

The authors would like to acknowledge the partial financial support provided by CNPq and AEB, both from Brasil.

6. REFERENCES

Amundsen, R.M., Dec, J.A., and Lindell, M.C., 2000, "Thermal Analysis Methods for an Earth Entry Vehicle", 11th Thermal and Fluids Analysis Workshop, Cleveland, August.

Bouilly, J.M., Euzen, M, Labaste, V., Mignot, Y., and Gerrekens, P., 1998, "Design of Thermal Protection Systems for Reentry Vehicles. A Survey of Calculation and Characterization Techniques Used by Aerospatiale", J. Space Technology, V. 18, no.3, pp.99-108.

Chen, Y.K. and Milos, F.S., 1999, "Ablation and Thermal Response Program for Spacecraft Heatshield Analysis", J. Spacecraft & Rockets, V.36, no.3, pp.475-483.

Cotta, R.M., 1993, "The Integral Transform Method in Computational Heat and Fluid Flow", CRC Press, FL, USA.

Cotta, R.M., 1998, "The Integral Transform Method in Thermal and Fluids Science e Engineering". Begell House, NY.

Cotta, R.M., Mikhailov, M.D., 1997, Heat Conduction: Lumped Analysis, Integral Transforms, Symbolic Computation, John Wiley, NY.

Cotta, R.M., Toro, P.G.P. and Machado, H.A., 1992, "Analytical Model for Aerodynamic Heating of Space Vehicles in Hypersonic Flow: Stagnation Region Analysis with Ablative Protection," Proc. of the 4th National Thermal Sciences Meeting – ENCIT 92, 137-140, Rio de Janeiro, Brasil.

Cotta, R. M., Falkenberg, C. V., Ruperti Jr., N.J., and Jian, Su, 2001, "Thermal Protection System Simulation for Atmospheric Reentry: - Engineering Models", 2nd Workshop on Research and Applications with *Mathematica*, II WARM, in: 2nd International Conference on Computational Heat and Mass Transfer, CHMT-2001, Rio de Janeiro, Brazil, October 2001.

Cotta, R. M., Falkenberg, C. V., Ruperti Jr., N.J., and Jian, Su, 2004, "Engineering Analysis of Ablative Thermal Protection for Atmospheric Reentry:- Improved Lumped Formulations and Symbolic-Numerical Computation", Heat Transfer Engng., Vol.25, no.6, pp.1-12.

Cotta, R.M., et al., 2006, Caracterização Termomecânica e Análise de Desempenho de Materiais de Proteção Térmica em Altas Temperaturas, Relatório Final, Programa Uniespaço, AEB, Dezembro.

Diniz, A.J., Aparecido, J.B., and Cotta, R.M., 1990, "Heat Conduction with Ablation in a Finite Slab", Heat and Tecnology, Vol.8(3-4).

Gomes, F.A.A., Campos Silva, J.B., Diniz, A.J., 2006, "Fomulation of the Ablation Thermal Problem in a Unified Form", J. Spacecraft & Rockets, Vol.43, no.1, pp.236-239.

Hindmarsh, A. C., 1983, "ODEPACK, A Systematized Collection of ODE Solvers, in Scientific Computing, R. S. Stepleman et al. (eds.), North-Holland, Amsterdam, pp. 55-64.

Hogge, M. and Guerrekens, P., 1982, "One-Dimensional Finite Element Analysis of Thermal Ablation with Pyrolysis", Computer Methods in Applied Mechanics and Engineering, Vol.33, pp.609-634.

Leiroz, A.J.K. and Cotta, R.M., 1990, "Convergence Enhancement of Eigenfunction Expansions for Nonhomogeneous Elliptic Diffusion Problems", Proc. of the III Encontro Nacional de Ciências Térmicas, ENCIT 90, pp.335-340, SC.

Ruperti, N.J., and Cotta, R.M., 1991 "Heat Conduction with Ablation in Multilayered Media", Proc. of the 11th Brazilian Congress of Mechanical Engineering, XI COBEM, São Paulo, SP (Brasil).

Ruperti Jr., N. J., and Cotta, R. M., 2000, "An Improved Lumped Differential Approach for the Solution of Thermal Ablation Problems", 8th Brazilian Congress of Thermal Sciences and Engineering, ENCIT 2000, Porto Alegre, Brasil.

Scofano Neto, F., Cotta, R.M., and Mikhailov, M.D., 1990, "Alternative Approach to the Integral Transform Solution of Nonhomogeneous Diffusion Problems", Int. Conf. on Advanced Computational Methods in Heat Transfer, V. 1, pp. 39-50, Southampton, UK.

Sias, D.F., Ruperti Jr., and R.M. Cotta, "Otimização de Algoritmo de Transformação Integral em Problemas de Ablação na Plataforma *Mathematica*", Proc. of the 4th Workshop on Integral Transforms and Benchmark Problems – IV WIT, CNEN, Rio de Janeiro, RJ, August 2005.(CD Rom)

Sias, D.F., N. Ruperti Jr., N., and Cotta, R.M., 2007, "Enhanced Convergence of Integral Transform Solution of Ablation Problems", Proc. of the 19th Brazilian Congress of Mechanical Engineering, XIX COBEM 2007, Brasilia, DF (Brazil)

Tauber, M.E., 1989, "A Review of High-Speed, Convective, Heat Transfer Computation Methods", NASA Technical Paper #2914.

Wolfram, S., 2005, "*The Mathematica Book*", 5th edition, Addison-Wesley/Wolfram Media.

7. RESPONSIBILITY NOTICE

The authors are the only responsible for the printed material included in this paper.